J. Iron Steel Res. Int. (2023) 30:1675–1686
https://doi.org/10.1007/s42243-022-00896-z

ORIGINAL PAPER

Optimization of iron ore blending based on replacing Australian low alumina limonite

Bin Li[1,2] · Heng Zhou[1] · Jian Huang[3] · Zong-wang Zhang[1] · Xue-feng She[1] · Jian-fang Wang[4] · Sheng-li Wu[1] · Ming-yin Kou[1]

Received: 18 May 2022 / Revised: 10 August 2022 / Accepted: 16 August 2022 / Published online: 6 February 2023

Abstract

Mauritanian iron ore powder (OM) has advantages of high iron grade, low aluminum content, and low loss on ignition, which can be used as a new mineral to replace low alumina limonite that has been exhausted in Australia. However, it will have a certain negative impact on sintering because of its high SiO_2 content. The mechanism of SiO_2 content affecting the sintering behavior was first studied through FactSage 7.2. Then, the liquid fluidity, penetration, and high-temperature performance of different iron ore powders were compared. Finally, the optimization of ore blending structure was studied by the micro-sintering method and the sinter pot test. The results show that the increase in SiO_2 content can reduce the assimilation temperature. The low penetration of OM can lead to an increase in the amount of liquid, and the high SiO_2 content of OM increases the viscosity of the liquid phase. What is more, the increase in SiO_2 also increases the formation of silicate and fayalite phase and inhibits the formation of silico-ferrite of calcium and aluminum (SFCA). To optimize ore blending structure, OM and the low SiO_2 powder OD from Australia were used together, which improves the content of SFCA by 2.04% and decreases the contents of calcium silicate and fayalite by 0.63% and 4.99%, respectively. The results of the sinter pot test indicated that the properties of sinter have been improved.

Keywords Mauritanian iron ore powder · Liquid fluidity · Penetration · Mineral composition · Sintering · Ore blending · Low alumina limonite

1 Introduction

With the rapid development of the global iron and steel industry, a large number of high-quality iron ore resources have been consumed like Yandi power, and the high-quality iron ore powder in each major iron ore supply area has decreased [1, 2]. Under this background, iron and steel enterprises began to use low-grade iron ore powder to adapt to the change in iron ore powder resources. The iron ore powder from Mauritania has the advantages of high iron grade and low aluminum content, which creates favorable conditions for its usage in sintering process [3, 4]. However, the high SiO_2 content may cause an increase in viscosity of the bonding phase, which adversely affects the liquid fluidity. At the same time, it will cause the increase in silicate and fayalite in the bonding phase, resulting in the inferior mineral bonding phase [5].

The optimization of ore blending technology in sintering is an effective method to improve the quality of sinter and efficient utilization of high silicon ore. The main method of ore blending optimization is based on the basic process performance of iron ore at high temperature [6–8]. For example, the assimilation and liquid fluidity of iron ore at high temperatures are critical indicators to measure the

✉ Heng Zhou
zhouheng@ustb.edu.cn

✉ Ming-yin Kou
koumingyin@ustb.edu.cn

1 State Key Laboratory of Advanced Metallurgy, School of Metallurgical and Ecological Engineering, University of Science and Technology Beijing, Beijing 100083, China

2 Shougang Jingtang Iron and Steel Co., Ltd., Tangshan 063200, Hebei, China

3 Key Laboratory of Knowledge Automation for Industrial Processes of Ministry of Education, School of Automation and Electrical Engineering, University of Science and Technology Beijing, Beijing 100083, China

4 Delong Iron and Steel Co., Ltd., Xingtai 054009, Hebei, China

sintering performance of ore. Some scholars evaluated the flow characteristics of samples by changing the vertical projection area of iron ore before and after sintering [9–11]. Some scholars also evaluated the degree of reaction between the original melt and iron ore by placing 15 wt.% CaO and Fe_2O_3 chemical reagent on the pressed iron ore sheet [12–14]. These works are useful for understanding the optimization of ore blending based on replacing Australian low alumina limonite. On the other hand, the composition of iron ore, like SiO_2, one of the main components of gangue, has an important influence on the sintering process. Many researchers have studied the influence of SiO_2 on sintering. For example, with the increase in SiO_2 content, the bonding phase would produce more unevenly distributed fayalite phases. And the content of silico-ferrite of calcium and aluminum (SFCA) and liquid phase in the bonding phase both decreased with the increase in SiO_2 content of iron ore powder at sintering temperature, while the content of silicate increased [15–17]. Besides, the increase in SiO_2 content will inevitably lead to an increase in CaO content under certain basicity conditions in sintering process [18, 19]. Because of excessive amounts of CaO in sinter, the decomposed CaO at outer layer will exist in the form of "white" and be absorbed by the sinter during the cooling process, which affects the strength of the sinter. Su et al. [20] found that with the increase in SiO_2 content, the liquid fluidity of the bonding phase decreased, and the content of minerals such as fayalite and calcium silicate increased. Yang et al. [21] studied the high-temperature basic characteristics and optimized ore blending of low silicon ore sintering blending.

The above studies have explained the changes in assimilation, liquid fluidity, and mineral composition of sinter bonding phase after the increase in SiO_2 content, but have not analyzed the mechanism of the changes. Zhai et al. [22] analyzed the influence of chemical composition on liquid fluidity and maximum penetration depth, especially for SiO_2 and Al_2O_3 contents, but the influence of coarse ore on liquid fluidity and penetration was not considered. Due to the high SiO_2 content, low Al_2O_3 content, and low loss on ignition (LOI) characteristics of Mauritanian iron ore powder (OM), the influence of OM on the high-temperature performance during the sintering process needs to be studied.

In this paper, firstly, the effect of SiO_2 on liquid fluidity was studied by FactSage 7.2. Then, the high-temperature characteristics of five kinds of mineral powders including OM and Yandi powder were analyzed, especially the high-temperature behavior changes of bonding phase after each iron ore powder replaced Yandi powder one by one. Finally, the optimized ore blending scheme with OM instead of Yandi power was investigated. Relevant research can provide technical support for the optimization of ore blending to reduce Yandi powder in industrial production.

2 Experimental

2.1 Materials

In this study, one kind of OM and four kinds of Australian iron ore powders (OA–OD) are used as the main raw materials. OM is magnetite from Mauritania, OB is Yandi powder, OA and OC are limonite, and OD is hematite. The OE and OF are hematite from Brazil, and OG was iron concentrate from Canada. The chemical compositions of each iron ore powder are shown in Table 1. In terms of chemical composition, the SiO_2 content of OM is much higher than that of the four Australian ore powders, but the LOI of OM is the lowest. There is no significant difference in SiO_2 content in four kinds of Australian iron ore powders, but the LOI of OC and OD is lower than that of the other two kinds of Australian ore powders.

2.2 Methods

2.2.1 Flow test of liquid phase

Liquid fluidity refers to the flow capacity of iron ore powder after the iron ore powder is turned into the liquid phase at a high temperature. It reflects the ability of iron ore powder to flow and bond surrounding materials in the sintering process after the iron ore powder reacts with CaO to generate a liquid phase [23]. According to the actual production in a steel plant, the fraction of CaO in adhesive powder is about 15 wt.%. Therefore, 1.0 g of fine mixed ore powder with 15 wt.% CaO was taken and pressed into a sample with a diameter of 8 mm by a press machine. The sample was placed on a platform for the sintering test using a micro-sintering equipment. The sintering equipment and heating system are shown in Fig. 1. The maximum temperature in the insulation stage is set at 1300 °C. First, air is inlet from room temperature to 600 °C. In order to protect the reaction device and extend its service life, nitrogen is injected to protect it when the reaction temperature rises to 600 °C in the test, and then, air will be injected again in the cooling process when the reaction temperature is below 1300 °C.

Liquid fluidity refers to the relation between the vertical projection area after sintering flow and the original vertical projection area before sintering, as shown in Eq. (1).

$$\mathrm{LDF} = (S_1 - S_2)/S_2 \tag{1}$$

Table 1 Chemical compositions and major minerals of iron ores

Iron ore	Chemical composition/wt.%					Major mineral
	TFe	SiO_2	Al_2O_3	MgO	LOI	
OM	62.71	8.88	0.86	0.50	0.08	Magnetite and hematite
OA	58.34	4.55	1.49	0.10	10.21	Goethite and hematite
OB	56.56	6.39	1.74	0.11	10.76	Goethite and hematite
OC	57.95	5.67	2.58	0.09	7.34	Goethite and hematite
OD	61.85	4.67	2.55	0.13	3.42	Hematite
OE	65.13	1.63	1.35	0.05	3.29	Hematite
OF	63.19	7.38	0.67	0.14	1.07	Hematite
OG	66.26	4.47	0.27	0.19	0.11	Magnetite

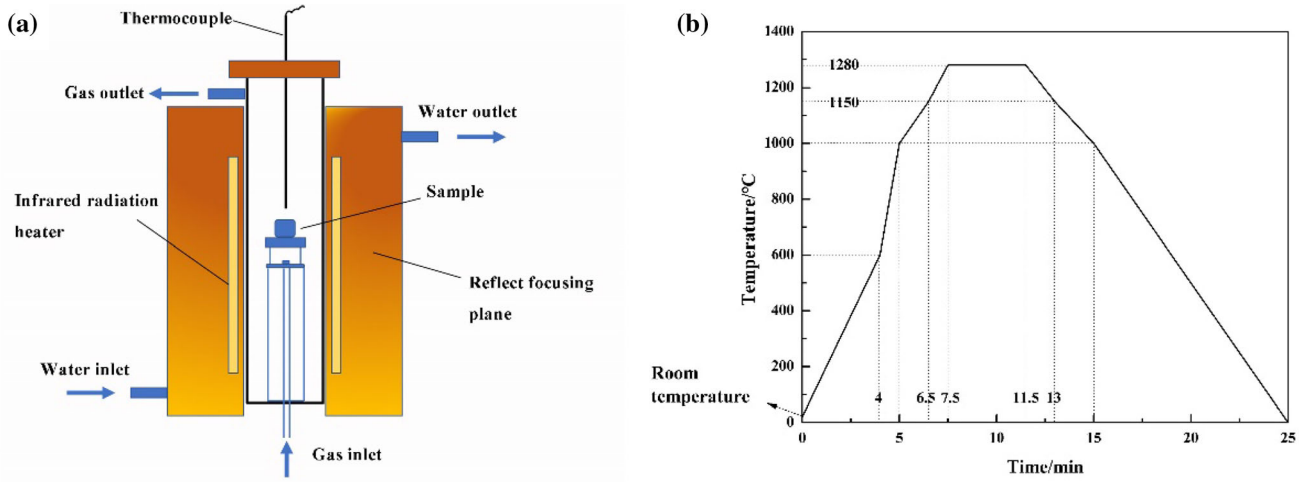

Fig. 1 High-temperature micro-sintering furnace (**a**) and heating system of micro-sintering test (**b**)

where LDF is the index of liquid fluidity; S_1 is the fluid area after high-temperature experiment, mm^2; and S_2 is the original area before high-temperature experiment, mm^2.

2.2.2 Penetration test of liquid phase

To clarify the difference in high-temperature reaction property of the bonding phase to different kinds of coarse particles, tests on the penetration of five kinds of iron ore powders were carried out. Penetration refers to the ability of coarse iron ore particles to react with the initial liquid phase generated by adhesive powder, which is characterized by the depth of penetration [22]. The pure reagents Fe_2O_3 and CaO were mixed in a molar ratio of 1:1, kept at 900 °C for 1 h in an air atmosphere, then heated to 1200 °C for 8 h, and then cooled to room temperature. 0.2 g SFCA powder was pressed into small cake samples with a diameter of 8 mm. Coarse particles of iron ore powder with a diameter of about 12.5 mm are washed, dried, and polished with sandpaper. The pressed cake sample was placed on the surface of coarse iron ore powder and sintered in a micro-sintering test device. Sintering temperature rise system and atmospheric condition are consistent with fluidity measurement. The sintered samples were mounted in epoxy resin and then dissected perpendicular to the interface. To obtain a smooth surface, the samples were ground with abrasive papers and polished with diamond pastes. The depth of high-temperature liquid penetration was measured by image analysis software, and the schematic of the liquid penetration test is shown in Fig. 2.

2.2.3 *K* value method

The "*K* value method" is a traditional semi-quantitative analysis method of the physical phase. Its basic principle is to add a reference substance (corundum) to the object to be tested to form a new mixed phase that meets the reference phase and measures the integral intensity of the strongest peak of the two phases. According to Eq. (2), the mass fraction of the phase to be measured in the new mixed

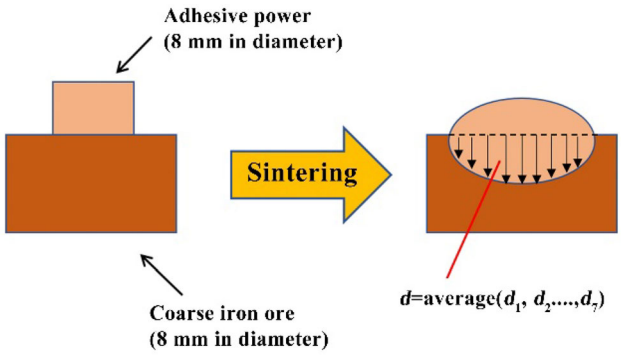

Fig. 2 Schematic of liquid penetration test. d—Average depth of liquid penetration; d_1, …, d_7—depth at some particular points

phase is calculated, and then, the mass fraction of the phase to be measured in the original sample is obtained.

$$\frac{I_a}{I_b} = K \cdot \frac{W_a}{W_b} \tag{2}$$

where I_a is the diffraction intensity of the strongest peak of the phase to be measured; I_b is the diffraction intensity of the strongest peak of the reference phase; K is the strength ratio between the pure phase to be measured and the reference phase, which is regarded as "reference strength" and usually expressed as "I/IC" on PDF cards; W_a is the mass fraction of the phase to be measured in the new mixture; and W_b is the mass fraction of the reference phase in the new mixture.

3 Results and discussion

3.1 Effect of SiO_2 on assimilation and liquid fluidity

Since OM has a high SiO_2 content, a chemical reagent was used to simulate actual iron ore powder to investigate the effect of SiO_2 content on assimilation and liquid fluidity. The chemical compositions of the adhesive powder are shown in Table 2, and the results of assimilation and liquid fluidity of the bonding phase at different SiO_2 contents are shown in Fig. 3.

As can be seen from Fig. 3, the assimilation temperature and liquid fluidity of the bonding phase both decrease to a certain extent with the increase in SiO_2, and the possible reason is that the increase in SiO_2 content promoted the formation of compounds with low melting points including $2CaO{\cdot}SiO_2$–$CaO{\cdot}Fe_2O_3$–$CaO{\cdot}2Fe_2O_3$, leading to the drop of the assimilation. To better understand the effect of SiO_2 content on the liquid phase of the bonding phase, the "Equilib" module in FactSage 7.2 was used for simulation and calculation. In the bonding phase with $W_{Fe_2O_3}:W_{CaO}$ = 3:1, the liquid phase changes in the SiO_2–Fe_2O_3 system phase diagram with the increase in SiO_2 content, and the simulation results are shown in Fig. 4. When the SiO_2 content increases from 4 wt.% (point A) to 6 wt.% (point B), the liquidus tends to decrease, indicating that the temperature of complete melting at point B is lower than that at point A. When the temperature is reduced to 1300 °C, the composition of solid phase changes from point A to point A' and from point B to point B'. According to the lever principle, the amount of liquid phase generated at point B' is higher than that generated at point A'. The above results show that in a certain range, the increase in SiO_2 will reduce the melting temperature of the bonding phase, and the amount of liquid phase will increase. However, the increase in SiO_2 leads to the decrease in basicity and the increase in the viscosity of the liquid phase at the same time, resulting in the decrease in the liquid fluidity of the bonding phase.

With the increase in SiO_2 content, the basicity of the bonding phase gradually decreases and the viscosity gradually increases. The reasons are described as follows. With the increase in SiO_2 content, Si^{4+} will form more oxygen tetrahedrons (SiO_4^{4-}) and behave as a network former in calcium ferrite. Thus, the movement of a large number of ions including Si^{4+} ions in the network is restricted, which leads to an increase in the viscosity of the bonding phase. The results have been confirmed by Saito et al. [24] and Machida et al. [25].

$$2CaO(s) + SiO_2(s) \rightarrow 2CaO \cdot SiO_2(s) \tag{3}$$

$$2CaO \cdot Fe_2O_3(s) + SiO_2(s) \rightarrow 2CaO \cdot SiO_2(s) + Fe_2O_3(s) \tag{4}$$

$$2(CaO \cdot Fe_2O_3) + SiO_2(s) \rightarrow 2CaO \cdot SiO_2(s) + 2Fe_2O_3(s) \tag{5}$$

From the thermodynamic point of view, the Gibbs free energy of reactions (3)–(5) is 133.6, − 76.95 and − 62.01 kJ mol^{-1}, respectively. With the increase in SiO_2 content, the transition from the calcium ferrite phase to the calcium silicate phase will be accelerated. The melting temperature of calcium ferrite is higher than that of calcium silicate; thus, excessive SiO_2 will also reduce the basicity of the bonding phase, which has a certain inhibitory effect on the formation of the liquid phase. In conclusion, it is necessary to maintain a proper SiO_2 content during sintering process.

3.2 Comparison of liquid fluidity and penetration of different iron ore powders

The liquid fluidity and the assimilation of five kinds of iron ore powders OM, OA, OB, OC and OD were tested. The assimilation of iron ore powder refers to the ability of iron

Table 2 Chemical compositions of adhesive powder

Scheme	Chemical composition/wt.%								R_2
	Fe_3O_4	Fe_2O_3	SiO_2	CaO	Al_2O_3	MgO	P_2O_5	Total	
Si-1	4.76	91.82	1.06	0.33	1.74	0.15	0.14	100	0.313
Si-5	4.57	88.12	5.05	0.32	1.67	0.14	0.13	100	0.063
Si-8	4.43	85.38	8.00	0.31	1.62	0.14	0.13	100	0.039

$R_2 = W_{CaO}/W_{Fe_2O_3}$

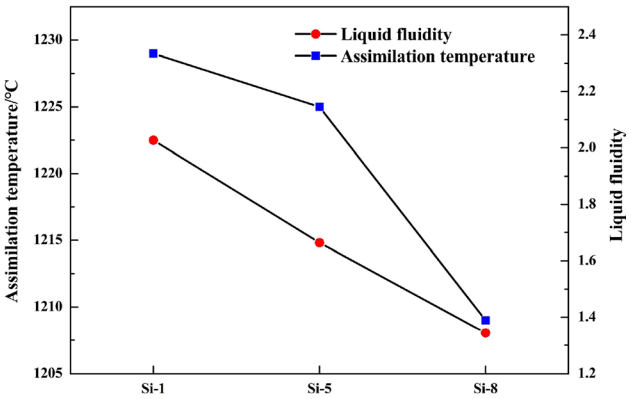

Fig. 3 Changes in assimilation temperature and liquid fluidity with SiO_2

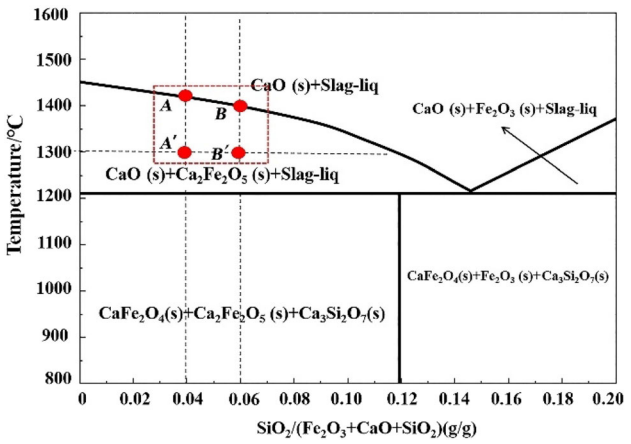

Fig. 4 Change of liquid phase of different components in SiO_2–Fe_2O_3 system phase diagram

ore powder to react with CaO to form a liquid phase, which is characterized by the lowest assimilation temperature. Assimilation temperature and liquid fluidity of iron ore powders are shown in Fig. 5.

As we can see from Fig. 5, the assimilation temperatures of OM and OA are lower, and the assimilation temperature of OA is lower than that of OM; the assimilation temperatures of OB and OD are roughly the same and higher than that of OM; OC has the highest assimilation temperature. The order of assimilation temperature from high to low is OC > OB > OD > OM > OA. The assimilation temperature of Australian iron ore powder is generally higher, while the assimilation temperature of OM is lower because it contains a high SiO_2 content. When the SiO_2 content of iron ore powder is high, the formation of low-melting point compounds will be promoted in the process of sintering, and the generation temperature of the liquid phase will be reduced.

In terms of liquid fluidity, OM has better liquid fluidity, which is higher than OB and OC, but lower than OA and OD. The order of liquid fluidity from high to low is OD > OA > OM > OB > OC. The liquid fluidity of OA and OB of the two limonites is roughly the same, while that of OC is much lower than that of the other four ores. The reason is that the viscosity of the bonding phase of iron ore powder increases significantly due to the high contents of SiO_2 and Al_2O_3 in OC. The assimilation temperature of OC was higher, and the liquid fluidity of OC was poor when the heating temperature was the same. Although the SiO_2 content of OM is high, it can still maintain good liquid fluidity. On the one hand, the assimilation temperature of OM is low. Although the increase in SiO_2 content increases the liquid viscosity to a certain extent, the superheat of the bonding phase increases and the liquid viscosity decreases at the same sintering temperature, which makes the liquid

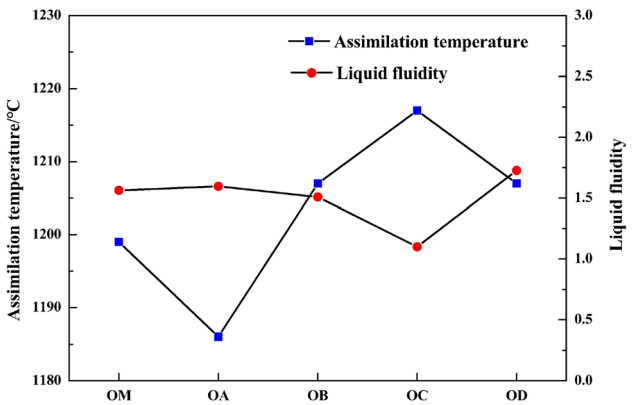

Fig. 5 Comparison of liquid fluidity and assimilability of iron ore powders

fluidity enhance. On the other hand, the increase in SiO_2 content will increase the production of liquid phase in the high-temperature sintering process to a certain extent, so as to improve the flow capacity of the bonding phase. High fluidity means that the range of surrounding materials is larger, which can improve the strength of the sinter effectively [26–28].

Besides, the liquid fluidity of iron ore powder is also closely related to the penetration of iron ore powder. In this study, five kinds of iron ore powders were tested for liquid penetration at high temperatures. The section morphology of coarse iron ore powders after liquid penetration is shown in Fig. 6. The horizontal lines in Fig. 6 show the upper surface of the coarse particles, and the curves show the boundary of liquid permeation [22, 26].

Figure 7 shows the depth of penetration and its relationship with LOI of each iron ore. As we can see, the liquid penetration depth of limonite is significantly greater than that of hematite, and the liquid penetration depth of limonite OA is greater than that of OB. The penetration depth of OM is smaller than that of Australian hematite OD, and the penetration depth of OM is lower than that of the other three Australian iron ore powders. The order of liquid penetration depth from large to small is OA > OB > OC > OD > OM.

With the increase in LOI, the depth of penetration gradually increases. This is because the LOI is positively correlated with the porosity. When the porosity of coarse particles increases, the capillary effect of stomatal channels is strengthened, so that more liquid phase penetrates into coarse particles during sintering and increases the depth of liquid penetration. Wu et al. [29] believed that when the coarse particles of iron ore powder had strong liquid penetration, the coarse particles would react with the primary liquid phase to generate the second liquid phase in the sintering reaction process, and the second liquid phase had high viscosity, which made the granulating effect worse and thus reduced the strength of sinter. This also explains that although OM has a high SiO_2 content and the viscosity of the liquid phase decreases to a certain extent, it has a large amount of liquid phase under high temperature, and the liquid phase is not easy to penetrate into the coarse particles of iron ore powder; thus, there is a more effective liquid phase, and OM has a strong liquid fluidity. Therefore, the optimal ore blending scheme of OM with strong penetration ore such as OC and OD can be considered to weaken the negative effect of strong penetration ore powder in the sintering process.

3.3 Comparison of high-temperature performance with different iron ore powders replacing OB

Based on the principle of improving the liquid fluidity of adhesive powder and inhibiting the high-temperature liquid penetration of coarse iron ore powder particles [30], the influence of adding different iron ore powders on the mineral composition of the bonding phase of mixed ore was studied based on the existing ore blending structure of an iron and steel enterprise. The influence of different iron

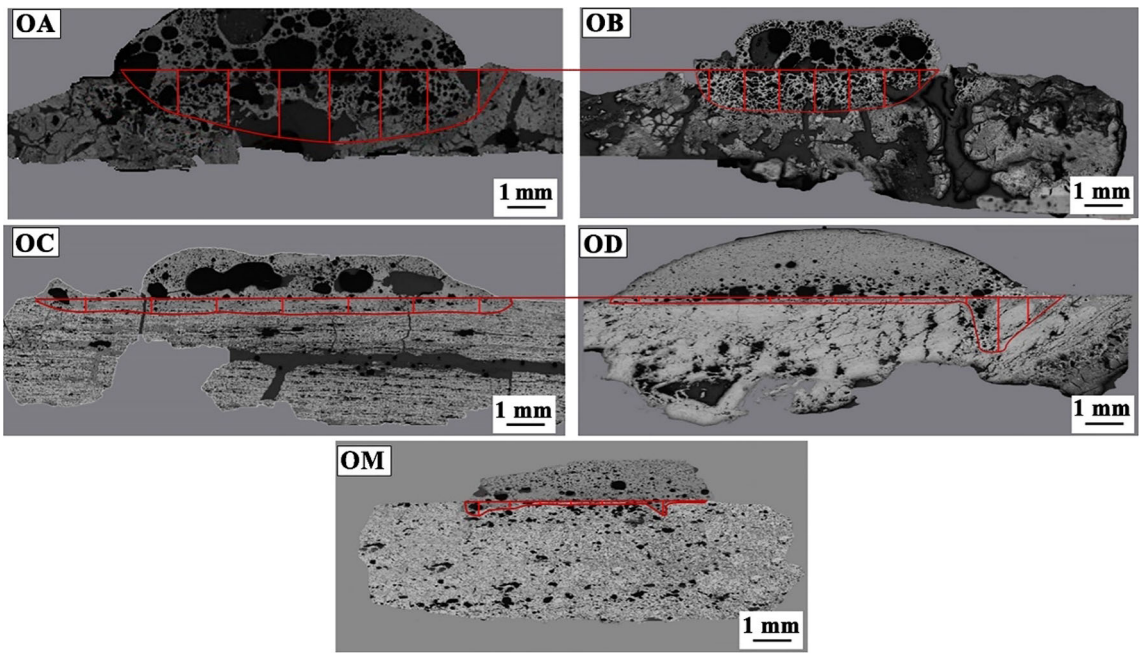

Fig. 6 Cross section morphology of iron ore powder coarse particles after liquid penetration

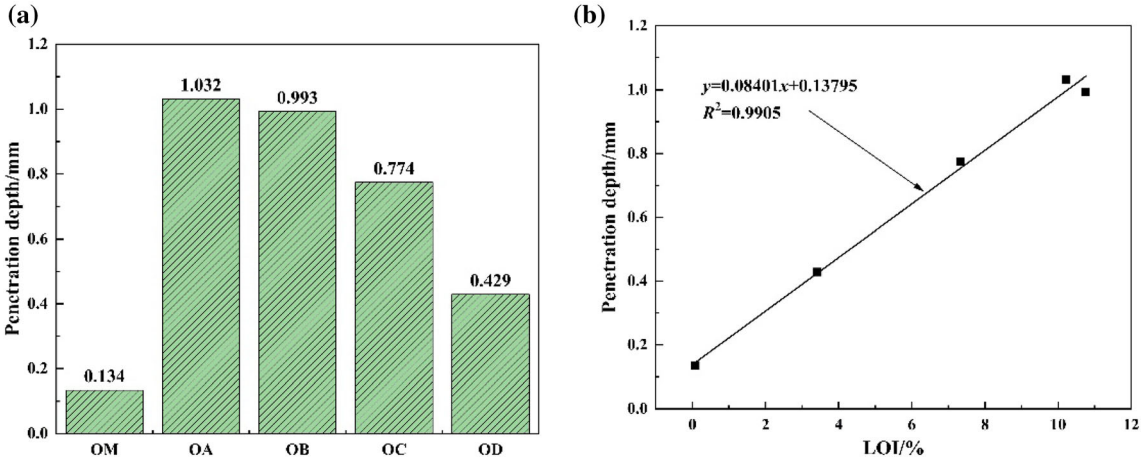

Fig. 7 Depth of penetration (**a**) and relationship with LOI (**b**) of each iron ore. R^2—Determination coefficient

ore powder ratios on mineral compositions was investigated by using OM, OC, and OD instead of OB, respectively. The ore blending structure of each scheme is shown in Table 3, and its chemical composition is shown in Table 4. The assimilation temperature and liquid fluidity of the bonding phase are shown in Fig. 8.

Compared with the Base case, the liquid fluidity index of scheme I and scheme III increased by 1.21 and 1.29, respectively, and the fluctuation of assimilation temperature is small. In scheme II, the assimilation temperature increased by 9 °C, and the liquid fluidity index decreased by 0.6. It can be seen that the assimilation and liquid fluidity of scheme II became worse, while scheme I and scheme III had little change in high-temperature properties.

X-ray diffraction (XRD) analysis was performed on the test samples, and the "*K*-value method" [31] was used to conduct semi-quantitative analysis on the XRD patterns. The PDF card numbers of minerals formed in bonding phase are shown in Table 5. The mineral compositions of the test samples under different schemes were obtained, as shown in Fig. 9 and Table 6. SFCA is a solid solution and does not have a certain composition. The chemical composition of SFCA in this study is shown in Table 7.

It can be seen from Table 6 that for scheme 2, the content of SFCA in the bonding phase decreased by 4.05%, while the high-aluminum brittle minerals in the bonding phase increased by 8.13%, which would reduce the strength of the sinter; thus, the amount of OC should be reduced as much as possible in the mixed ore. For scheme I, although the content of high-aluminum brittle minerals in the bonding phase decreased by 1.54%, the content of SFCA also decreased by 5.67%, while the contents of calcium silicate and fayalite increased by 2.44% and 0.06%, respectively. As for scheme III, the content of SFCA in the bonding phase increased by 1.31%, and the content of silicate and fayalite was both lower than the Base case. Based on the principle of complementary iron ore properties, OM and OD can be considered to replace OE together.

At the same time, we analyzed the mechanism of the mineral compositions of the bonding phase via the change of SiO_2 and Al_2O_3 contents in the sinter. From the phase diagram of the CaO–Fe_2O_3–SiO_2 ternary system (Fig. 10), we can also see that the mineral compositions of the bonding phase are different from point *A* to point *C* in the process with the increase in SiO_2 content. It can be seen that with the continuous increase in SiO_2 content, $2CaO{\cdot}SiO_2$ (C_2S) and $CaO{\cdot}SiO_2$ (CS) began to precipitate in the bonding phase, indicating that the increase in SiO_2 content in the bonding phase does promote the generation of silicate and decrease calcium ferrite content relatively.

To better understand the initial phase, we calculated the phase composition at 1280 °C using the 'balance' module

Table 3 Ore blending structure of OB replaced by different iron ore powders (including miscellaneous auxiliary materials) (wt.%)

Scheme	OB	OM	OC	OD	OA	OE	OF	OG	Auxiliary material	Total
Base	19.00	0	15.00	0	28.00	15.00	5.00	10.00	8.00	100.00
I (OM replacing OB)	0	19.00	15.00	0	28.00	15.00	5.00	10.00	8.00	100.00
II (OC replacing OB)	0	0	34.00	0	28.00	15.00	5.00	10.00	8.00	100.00
III (OD replacing OB)	0	0	15.00	19.00	28.00	15.00	5.00	10.00	8.00	100.00

Table 4 Chemical composition of fine powder of mixed ore (including miscellaneous auxiliary materials)

Scheme	Chemical composition/wt.%					R_2
	TFe	SiO_2	CaO	Al_2O_3	MgO	
Base	60.10	4.68	0.30	1.55	0.13	0.063
I	61.29	5.16	0.35	1.38	0.20	0.068
II	60.37	4.54	0.30	1.71	0.13	0.066
III	61.12	4.35	0.30	1.71	0.13	0.069

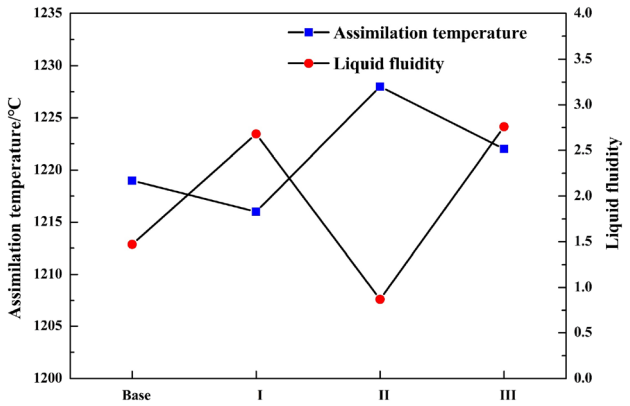

Fig. 8 Assimilation temperature and liquid fluidity of bonding phase

Table 5 PDF card numbers of minerals formed in bonding phase

Mineral	Formula	PDF card number
SFCA	$Ca(Fe_{1.4}Al_{0.6})SiO_6$	25-0143
Magnetite	Fe_3O_4	19-0629
High-aluminum brittle mineral	$Ca_{12}Al_{14}O_{33}$	09-0413
Calcium silicate	$Ca_3Si_2O_7$	22-0539
Hematite	Fe_2O_3	33-0664
Fayalite	$(Mg,Fe)_2SiO_4$	31-0795

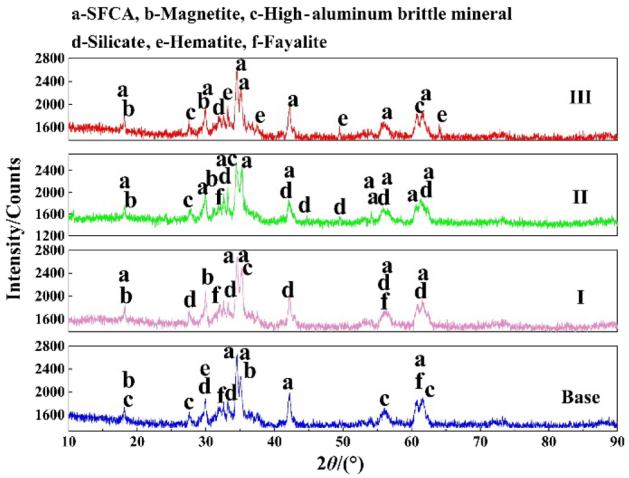

Fig. 9 XRD patterns of bonding phase under different schemes. 2θ—Diffraction angle

of FactSage 7.2. From the phase diagram of the CaO–Al_2O_3–SiO_2 ternary system (Fig. 11), comparing the phase composition of point *A* and point *B*, point *A* is pure quartz, and point *B* also generates the anorthite and mullite phase except with the tridymite phase. The change shows that in the case of liquid containing SiO_2 content, these three phases will generate aluminate once with the addition of CaO and Al_2O_3 in the liquid phase. It can be seen from Fig. 12 that when the contents of CaO and Al_2O_3 in the liquid phase reach a certain amount, gehlenite phase will be generated. And the compressive strength of gehlenite is 12,963 Pa, and the compressive strength of anorthite is 12,346 Pa, both of which are high-aluminum brittle minerals. Therefore, when the content of Al_2O_3 in the bonding phase increases, it will react with calcium to form brittle minerals, leading to the decline of the bonding strength [32–34].

3.4 Optimization of ore blending structure adding with OM and OD

Because OC has a poor high-temperature property, while OB and OD are complementary to each other in high-temperature properties, the optimized ore blending scheme that replaces OE with OB and OD together was designed to investigate the change of high-temperature properties of mixed ore. The optimized ore blending scheme of blending is given in Table 8, and its chemical compositions are listed in Table 9. The assimilation temperature and liquid fluidity of the bonding phase are shown in Fig. 12.

We can see from Fig. 12 that the assimilation temperature of the optimized ore blending scheme III-1 is greatly reduced and lower than that of the Base case, which indicated that the assimilation of bonding phase is improved

Table 6 Mineral composition of sintering under different ore blending schemes (wt.%)

Scheme	SFCA	Magnetite	High-aluminum brittle mineral	Calcium silicate	Hematite	Fayalite	Total
Base	61.29	5.69	6.12	6.18	10.20	10.52	100.00
I	55.62	9.36	4.58	8.62	11.24	10.58	100.00
II	57.24	5.94	14.25	5.00	13.61	3.96	100.00
III	62.60	7.25	10.91	5.55	8.16	5.53	100.00

Table 7 Chemical composition of SFCA in this study (wt.%)

Fe	Si	Al	Ca	O
26.94	9.62	16.70	13.75	32.99

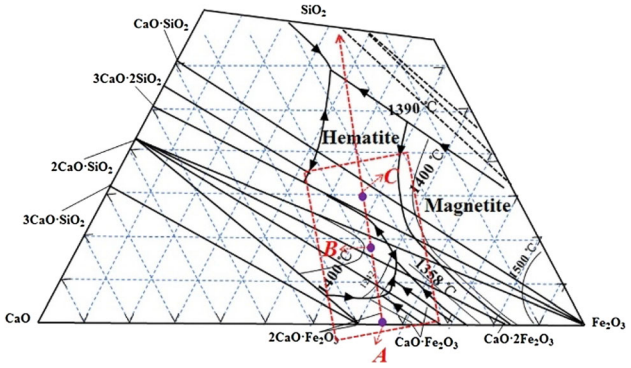

Fig. 10 Part of phase diagram of $CaO–Fe_2O_3–SiO_2$ ternary system

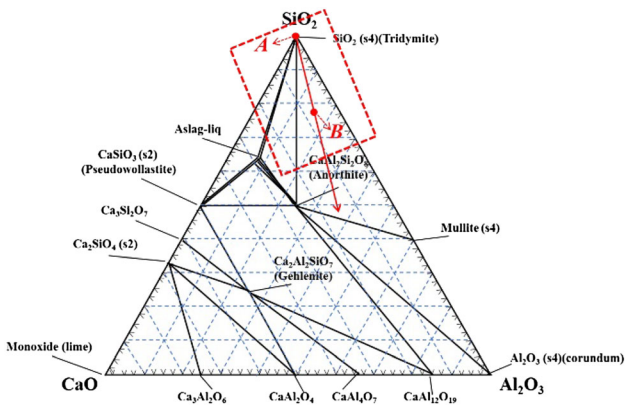

Fig. 11 Phase diagram of $CaO–Al_2O_3–SiO_2$ ternary system

after OE is replaced by OD and OE together. Because of the addition of a large amount of OM that contains a high SiO_2 content, the liquid fluidity of the bonding phase decreases, and it is still higher than that of the Base case.

We also tested the bonding phase by XRD. The results are shown in Fig. 13, and the mineral compositions of the bonding phase are shown in Table 10. As we can see, the

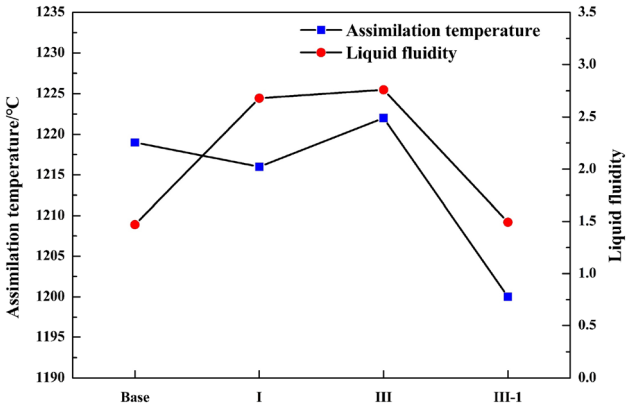

Fig. 12 Assimilation temperature and liquid fluidity of optimized bonding phase

content of SFCA in the bonding phase of scheme III-1 reaches 63.3%, the content of high-aluminum brittle minerals is higher than that of scheme I but lower than that of the Base case, and the contents of calcium silicate and fayalite are also lower than those of the Base case. It can be seen that the way that replaced OE with OM and OD improves the structure of the sinter indeed.

3.5 Sintering indexes of sinter pot test

According to the ore blending structure shown in Table 8, a certain proportion of ore return and flux (limestone, quicklime, dolomite, and serpentine) were added to verify the results through the sinter pot test, as shown in Table 11.

Through Table 11, we can find that scheme I has better assimilation and liquid fluidity with the addition of OM, but the granulating effect is poor in the process of sintering because its particle size is too fine. It is characterized that since the vertical sintering velocity (VSV) is too fast, the liquid phase reduces in the sintering process, and the bonding degrees between particles are insufficient; thus, the yield and tumbler index (TI) of the sinter are lower than those of the Base case. For scheme III-1, with the addition of OM and OD, the VSV, yield, TI, solid fuel consumption (SFC), and the productivity are improved. The OD has larger particle size and better liquid fluidity ability, which can better compensate for the poor granulation effect

Table 8 Structure of optimized mixed ore (wt.%)

Scheme	OB	OM	OC	OD	OA	OE	OF	OG	Auxiliary material	Total
Base	19.00	0	15.00	0	28.00	15.00	5.00	10.00	8.00	100.00
I	0	19.00	15.00	0	28.00	15.00	5.00	10.00	8.00	100.00
III	0	0	15.00	19.00	28.00	15.00	5.00	10.00	8.00	100.00
III-1 OM + OD replacing OB	0	10.00	15.00	9.00	28.00	15.00	5.00	10.00	8.00	100.00

Table 9 Chemical compositions of optimized mixed ore

Scheme	Chemical composition/wt.%					R_2
	TFe	SiO_2	CaO	Al_2O_3	MgO	
Base	60.10	4.68	0.30	1.55	0.13	0.063
I	61.29	5.16	0.35	1.38	0.20	0.068
III	61.12	4.35	0.30	1.71	0.13	0.069
III-1	64.11	5.01	0.34	1.61	0.18	0.069

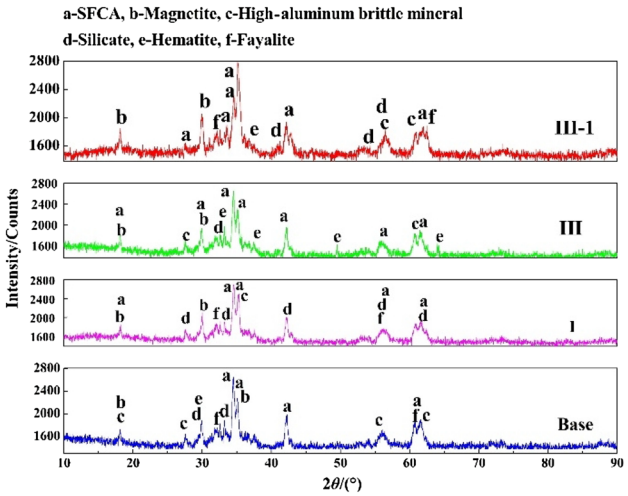

Fig. 13 X-ray diffraction patterns of bonding phase under different optimized schemes

caused by the fine-grained OM. Thus, the indexes of sinter pot were improved obviously. Figure 14 shows the microstructure of the bonding phase.

As we can see from Fig. 14, in the bonding phase of the Base case, the main minerals are SFCA phase and magnetite phase, with a small number of silicates and pores. The silicate phase is embedded in the bonding phase, and it is closely bonded with other minerals. In the bonding phase of scheme I, the amount of SFCA in the bonding phase decreases, and the amount of silicate minerals increases obviously due to the increase in the addition amount of OM. In the bonding phase of scheme III-1, a certain amount of OD is added based on OM. The main mineral in the bonding phase is the SFCA phase; not only does its quantity increase obviously, but also it is in the form of corrosion. In addition, magnetite and a small amount of

Table 10 Mineral composition of sinter under different optimized ore blending schemes (wt.%)

Scheme	SFCA	Magnetite	High-aluminum brittle mineral	Calcium silicate	Hematite	Fayalite	Total
Base	61.29	5.69	6.12	6.18	10.20	10.52	100.00
I	55.62	9.36	4.58	8.62	11.24	10.58	100.00
III	62.60	7.25	10.91	5.55	8.16	5.53	100.00
III-1	63.33	8.88	5.72	6.06	9.63	6.38	100.00

Table 11 Indexes of sinter pot test

Scheme	VSV/(mm min^{-1})	Yield/%	TI/%	Productivity/(t m^{-2} h^{-1})	SFC/(kg t^{-1})
Base	23.25	78.77	71.67	1.26	52.96
I	25.30	76.81	70.33	1.41	53.99
III	23.05	78.03	71.33	1.35	50.82
III-1	23.72	80.12	72.17	1.39	50.62

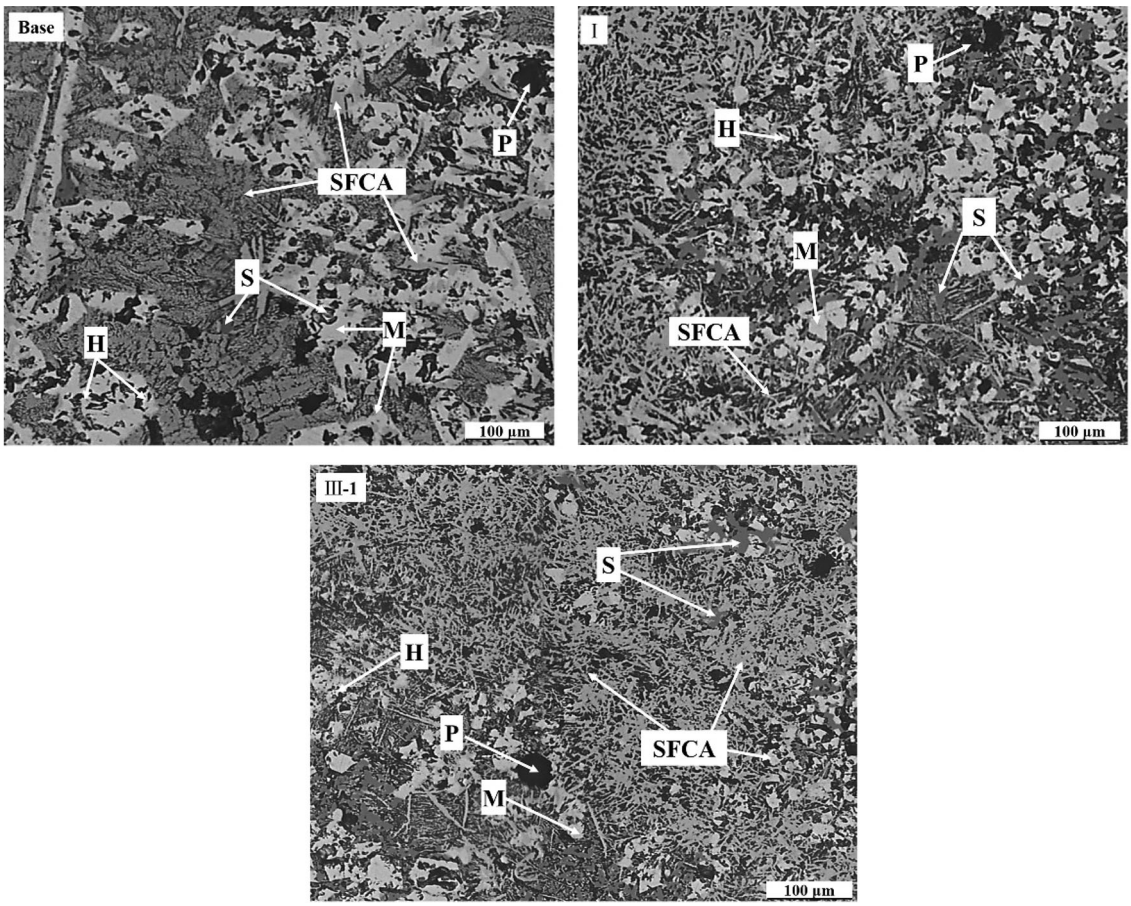

Fig. 14 Microstructure of bonding phase. H—Hematite; M—magnetite; P—pore; S—silicate

silicate are embedded around the liquid phase, which is conducive to the increase in sinter strength.

Based on the above research results, compared to the Base case, the assimilation and liquid fluidity of the bonding phase became better after OM and OD replaced OB together. Since the content of SFCA increases and the contents of silicate and fayalite decrease at the same time, the strength and reducibility of the sinter are good. Thus, Mauritanian iron ore powder OM can be used in the sintering with the addition of OD, and the properties of the sinter have been improved.

4 Conclusions

1. In terms of the influence of SiO_2 content on high-temperature property and mineral formation of bonding phase, the calculation results by FactSage 7.2 show that the increase in SiO_2 content reduces the assimilation temperature of the bonding phase, promotes the formation of liquid phase, and increases the liquid viscosity at the same time. On the other hand, the increase in SiO_2 content reduces the amount of SFCA in the bonding phase and promotes the formation of silicate and fayalite.

2. The high-temperature properties of iron ore powder produced from different areas are different. The order of liquid fluidity that is from high to low is OD > OA > OM > OB > OC, and the liquid fluidity of OM is higher than that of Yandi power OB because of the lower assimilation and the lower penetration, and while the order of penetration that is from high to low is OA > OB > OC > OD > OM. The liquid fluidity of OD is higher than that of OB, and there is little difference between OD and OB in assimilation temperature. The assimilation temperature of OC was higher than that of OB, and the liquid fluidity of OC was lower than that of OB.
3. Although the assimilation and liquid fluidity of OM are good, a certain amount of silicate and fayalite are formed, and the formation of SFCA in OD is good while a certain amount of high-aluminum brittle minerals will be formed at the same time. Based on the principle of complementary performance, OM and OD were added at the same time to replace OB. Compared to the Base case, SFCA content of bonding phase increased by 2.04%, while calcium silicate content and fayalite content decreased by 0.63% and 4.99%, respectively; thus, the properties of sinter were improved.

Acknowledgements The authors would like to thank the the National Key Research and Development Program of China (Grant Nos. 2021YFC2902400 and 2021YFC2902404) and the National Natural Science Foundation of China (Grant Nos. 51904023 and 51804027).

Declarations

Conflict of interest The authors have no relevant financial and non-financial competing interests.

References

[1] C.C. Yang, D.Q. Zhu, J. Pan, Z.Q. Guo, Iron and Steel 57 (2022) No. 5, 11–21.
[2] Y. You, J.B. Guo, G. Li, Z. Zheng, Y. Li, X.W. Lü, Int. J. Miner. Metall. Mater. 29 (2022) 2152–2161.
[3] B. De Waele, A. Aitken, M. Van Mourik, K.O. Laab, M.E.O.M. Yeslem, T. Mohamedou, ASEG Extended Abstracts 2019 (2019) 1–3.
[4] L. Ma, L.H. Cao, S.Q. Pei, H.J. Li, S.J. Wang, R.L. Li, Sinter. Pelletiz. 37 (2012) No. 4, 15–17.
[5] Z.Y. Ji, Y.J. Zhao, M. Gan, X.H. Fan, X.L. Chen, L. Hu, Minerals 9 (2019) 449.
[6] M.Y. Kou, Z. Zhang, W. Zeng, H. Zhou, S.L. Wu, Iron and Steel 57 (2022) No. 2, 1–11.
[7] F. Wang, J.F. Xiang, Y.F. Guo, F.Q. Zheng, J. Iron Steel Res. 32 (2020) 89–95.
[8] X.Y. He, Z.L. Liu, S.L. Wu, B. Zhao, F. Yang, Iron and Steel 57 (2022) No. 2, 28–35.
[9] J.J. Dong, G. Wang, Y.G. Gong, Q.G. Xue, J.S. Wang, Ironmak. Steelmak. 42 (2015) 34–40.
[10] X.L. Liu, S.L. Wu, W. Huang, K.F. Zhang, K.P. Du, ISIJ Int. 54 (2014) 2089–2096.
[11] S.L. Wu, H.P. Li, W.L. Zhang, B. Su, Metals 9 (2019) 404.
[12] M. Zhou, T. Jiang, S.T. Yang, X.X. Xue, Int. J. Miner. Process. 142 (2015) 125–133.
[13] M.Y. Kou, H.P. Li, S.L. Wu, B. Su, W.L. Zhang, Ironmak. Steelmak. 46 (2019) 199–205.
[14] W.J. Ni, H.F. Li, L. Shao, Z.S. Zou, ISIJ Int. 60 (2020) 662–673.
[15] J. Zhang, X.M. Guo, Y.H. Qi, D.L. Yan, J. Iron Steel Res. Int. 22 (2015) 288–296.
[16] N.A.S. Webster, M.I. Pownceby, I.C. Madsen, A.J. Studer, J.R. Manuel, J.A. Kimpton, Metall. Mater. Trans. B 45 (2014) 2097–2105.
[17] X. Lv, C. Bai, Q. Deng, X. Huang, G. Qiu, ISIJ Int. 51 (2011) 722–727.
[18] E. Kasai, Y. Sakano, T. Kawaguchi, T. Nakamura, ISIJ Int. 40 (2000) 857–862.
[19] L. Lu, Mining, Metallurgy and Exploration 32 (2015) 88–96.
[20] L.X. Su, S.L. Wu, X.B. Zhai, X.D. Ma, China Metallurgy 30 (2020) No. 1, 18–25.
[21] S.P. Yang, H.X. Sun, T.T. Zhang, S.M. Liu, H.J. Liu, J. Iron Steel Res. (2022) https://doi.org/10.13228/j.boyuan.issn1001-0963.20220246.
[22] X.B. Zhai, S.L. Wu, H. Zhou, L.X. Su, X.D. Ma, Ironmak. Steelmak. 47 (2020) 405–416.
[23] S.L. Wu, G.L. Zhang, S.G. Chen, B. Su, ISIJ Int. 54 (2014) 582–588.
[24] N. Saito, N. Hori, K. Nakashima, K. Mori, Metall. Mater. Trans. B 34 (2003) 509–516.
[25] S. Machida, K. Nushiro, K. Ichikawa, H. Noda, H. Sakai, ISIJ Int. 45 (2005) 513–521.
[26] S.L. Wu, X.B. Zhai, L.X. Su, X.D. Ma, J. Iron Steel Res. Int. 27 (2020) 755–769.
[27] J. Peng, L. Zhang, L.X. Liu, S.L. An, Metall. Mater. Trans. B 48 (2017) 538–544.
[28] M. Gan, X.H. Fan, Z.Y. Ji, X.L. Chen, L. Yin, T. Jiang, Z.Y. Yu, Y.S. Huang, Ironmak. Steelmak. 42 (2015) 351–357.
[29] S.L. Wu, B. Su, Y.H. Qi, M.Y. Kou, Y. Li, W.L. Zhang, Metall. Mater. Trans. B 48 (2017) 2469–2480.
[30] S.L. Wu, M.Y. Dai, D. Oliveira, Y.D. Pei, J. Xu, H.L Han, J. Univ. Sci. Technol. Beijing 32 (2010) 719–724.
[31] J.W. Huang, Z. Li, X-ray diffraction of polycrystalline materials: experimental principles, methods and applications, Metallurgical Industry Press, Beijing, China, 2012.
[32] T. Umadevi, R. Sah, P.C. Mahapatra, Miner. Process. Extr. Metall. 123 (2014) 75–85.
[33] L. Li, J. Liu, X. Wu, X. Ren, W. Bing, L. Wu, ISIJ Int. 60 (2010) 327–329.
[34] H.P. Li, S.L. Wu, Z.B. Hong, W.L. Zhang, H. Zhou, M.Y. Kou, Processes 7 (2019) 931.